coatings

MDPI

Article

Preparation of Polyurethane/Acrylate Composite Emulsion for Inkjet Printing

Xin Wang [1,2], Jimei Wu [1,3,*], Fuqiang Chu [2,*] and Yao Feng [1]

[1] School of Mechanical and Precision Instrument Engineering, Xi'an University of Technology, Xi'an 710048, China; wangxin@qlu.edu.cn (X.W.); fengyaoaaa2021@163.com (Y.F.)
[2] Faculty of Light Industry, Qilu University of Technology (Shandong Academy of Sciences), Jinan 250353, China
[3] School of Printing, Packaging Engineering and Digital Media Technology, Xi'an University of Technology, Xi'an 710048, China
* Correspondence: wujimei@xaut.edu.cn (J.W.); fqchu@qlu.edu.cn (F.C.)

Abstract: Water-borne polyurethane/acrylate (WPUA) emulsion was prepared through emulsion polymerization between vinyl terminated waterborne polyurethane (WPU) and methyl methacrylate (MMA) in this research. Thermogravimetric Analysis (TGA), transmission electron microscopy (TEM), contact angle analysis, and particle size distribution analysis were employed to investigate the performance of the prepared emulsion and coatings with various content of MMA content. The results demonstrated that the thermal resistance, water resistance, and hardness of the prepared WPUA coatings were enhanced by the introduction of the MMA monomer. The contact angle (CA) and particle size of WPUA emulsion increased with the increase of MMA content. Meanwhile, the water-borne inkjet printing ink was prepared using WPUA emulsion as binder resin, and the printing test result showed that the prepared inkjet ink has good printability and color rendering, indicating that WPUA emulsion has great application prospects in the field of inkjet printing.

Keywords: polyurethane; printability; inkjet printing

Citation: Wang, X.; Wu, J.; Chu, F.; Feng, Y. Preparation of Polyurethane/Acrylate Composite Emulsion for Inkjet Printing. *Coatings* **2022**, *12*, 1081. https://doi.org/10.3390/coatings12081081

Academic Editor: Günter Motz

Received: 28 June 2022
Accepted: 28 July 2022
Published: 31 July 2022

1. Introduction

In the context of energy shortages, reducing carbon emissions has become an important global issue [1,2]. Considering environmental factors, the solvent-based ink is gradually replaced by water-borne ink in the field of printing and packing due to the release of enormous volatile organic compounds (VOCs) during coatings formulation [3]. The demand for high-performance water-borne ink is to have excellent printability and coating performance [4]. Printability of ink is related to transfer and wetting characteristics such as viscosity, particle size, and surface tension, and coating performance is related to mechanical properties, hardness, and aging resistance [5–7].

As we all know, the comprehensive properties of water-borne ink depend on the binder resin [8]. Among the main binder resin raw materials, polyurethanes are one of the widely used polymers in the field of adhesives [9], leather [10], foaming agents [11], and elastomer [12] due to excellent properties such as flexibility, tensile strength, adhesion, and aging resistance [13,14]. In order to realize the dispersion of polyurethane into polar solvents such as water, hydrophilic monomers must be polymerized into polyurethane chains [15]. A usual approach to realize the dispersion of polyurethane into water is to induce hydrophilic groups such as carboxyl or sulfonic acid groups into the polyurethane backbone [16,17]. In spite of realizing the solubility of WPU in water, the existence of a hydrophilic group resulted in poor water and alkali resistance for WPU coating, which limited the applications in many fields [18]. An efficient way to achieve better performance of water-borne polyurethane (WPU) is to modify the polyurethane with other polymers.

Acrylates have excellent properties of hardness, water and chemical resistance, gloss, and thermal resistance [19]. Due to their high polarity and complete saturation, acrylates are widely used in adhesives, coatings, and sealants, and those advantages of acrylates can make up for the shortcomings of WPU [20,21]. Therefore, how to realize the synergy effect between polyurethane and acrylate has received enormous attention [22]. Physical blending and emulsion polymerization are two main approaches to combine the advantages of the two emulsions [23]. As physical blending, it is a convenient way to prepare polyurethane/acrylate hybrid emulsions, but the the progress of blending system performance is limited to the incompatibility of the two components [24]. Compared with physical blending, the emulsion polymerization method can achieve the compatibility of polyurethane and acrylate at the molecular levels. In this way, the synergy effect between polyurethane and acrylate is the maximum [25].

In this article, the WPUA emulsion was synthesized by emulsion polymerization. Firstly, the vinyl terminated waterborne polyurethane (WPU) was prepared according to the previous report. Secondly, the WPUA emulsion was prepared through the polymerization between vinyl terminated waterborne polyurethane (WPU) and methyl methacrylate (MMA) monomers. The morphology, particle size distribution, CA, thermal stability, and water absorption of WPUA emulsions and coatings were investigated. Meanwhile, the water-borne inkjet printing ink was prepared with WPUA emulsion as the binder resin, and the printability and color development ability of the inkjet ink were tested.

2. Materials and Methods

2.1. Materials

Vinyl terminated WPU emulsion (model: Urosin®4616) was purchased from Wanhua Chemical Group Co., Ltd. (Yantai, China). Methyl methacrylate (MMA), Sodium dodecyl sulfonate (SDS), potassium persulfate (KPS), and triethanolamine (TEA) of analytical pure grades were purchased from Shanghai Macklin Biochemical Co., Ltd. (Shanghai, China). Pigments such as cyan (C), magenta (M), yellow (Y), and black (K) were purchased from Yuhong Pigment Co., Ltd. (Dezhou, China). The wetting agent (Aquacer 497) was supplied by BYK (Konstanz, Germany). Deionized water was created in our laboratory. No reagents were purified before being used.

2.2. Methods

2.2.1. Preparation of WPUA Emulsion Using Semi-Bath Method

The WPUA emulsion was synthesized using a four-necked flask equipped with a mechanical string, nitrogen inlet, condensing reflux device, and thermometer. The metered WPU emulsion, MMA, and SDS were dropped into a flask and stirred for 30 min. The temperature of the reaction system was kept at 75 °C. The KPS solution was added dropwise to the flask with stirring. After adding the KPS solution, the system was kept at 75 °C for 30 min. The WPUA emulsion was prepared by adding TEA after the system was cooled to 25 °C. The recipes for preparing WPUA emulsion are illustrated in Table 1.

Table 1. The recipes for WPUA emulsion.

Sample	WPU (g)	Acrylates (g)	Initiator (g)	Emulsifier (g)
WPUA Emulsion	**WPU**	**MMA**	**KPS**	**SDS**
WPUA-10	50	5	0.05	0.1
WPUA-20	50	10	0.1	0.2
WPUA-30	50	15	0.15	0.3
WPUA-40	50	20	0.2	0.4

2.2.2. Preparation of WPUA Emulsion Using Bath Method

The WPUA emulsion was synthesized using a four-necked flask equipped with a mechanical string, nitrogen inlet, condensing reflux device, and thermometer. The metered WPU emulsion, MMA, SDS, and KPS were dropped into flask and stirred for 30 min. The temperature of the reaction system was kept at 75 °C for 4.5 h. The WPUA emulsion was prepared by adding TEA after the system was cooled to 25 °C.

The recipes for preparing WPUA emulsion using the bath method are also shown in Table 1.

2.3. Preparation of inkjet printing ink and C M Y K color blocks

The metered pigment, WPUA emulsion, wetting agent, and deionized water were dropped into a four-necked flask equipped with a mechanical stirrer and stirred for 0.5 h. Then, the mixture was filtered through a membrane with a pore size of 0.22 um, and the inkjet ink was obtained.

The inkjet printing color blocks such as cyan (C), magenta (M), yellow (Y), and black (K) were designed by Photoshop software (Adobe Photoshop CS5) and output onto coated paper with basis weight of 150 g/m^2 by an inkjet printer (Epson, SureColor P9080, Suwa, Japan) using the prepared ink.

2.4. Characterization

The morphology of emulsion particles was observed by transmission electron microscopy (JEOL, JEM-F200, Tokyo, Japan). The particle size distribution of the emulsion was tested by particle size analyzer (Malvern, Nano ZS, Malvern, England). The thermal resistance of the coating was measured by thermogravimetric analysis (TGA Q50, TA Instruments, New Castle, DE, USA). The contact angle analyzer (KRUSS, DSA100, Hamburg Germany) was used to measure the static droplet contact angle of the emulsion onto the neat glass slide without any treatment. The contact angle value of the emulsion was calculated by the software that came with the contact angle analyzer. A spectrophotometer (X-Rite, eXact, Grand Rapids, MI, USA) was used to measure the chromatic aberration (ΔE) of the prepared color blocks. We set a random point in the color block as the reference point and recorded the color information of this point with the spectrophotometer. Then, 20 points at different positions in the color block were selected and we recorded each color's information with spectrophotometer. ΔE between the 20 selected points and the reference point was calculated by the software that came with the spectrophotometer respectively. Finally, ΔE of the prepared color blocks was obtained by taking the average of the ΔE about the 20 selected points and the reference point. All the measurements were carried out under D65 standard light source conditions. The thermogravimetric analysis of the coating was performed using a thermogravimetric analyzer. The sample (3–4 mg) was placed in a platinum pan and heated under N_2 atmosphere (50 mL/min), at a heating rate of 10 °C/min rising from room temperature to 500 °C. The water absorption of the coatings was calculated by the flowing calculation, Formula (1):

$$W = \frac{M_2 - M_1}{M_1} \quad (1)$$

W (%): Water absorption of the coating.

M_1 (g): The initial weight of the coating which is cut into pieces (1 cm × 1 cm), and the thickness of coating piece is about 2 mm.

M_2 (g): Weight of the piece after soaking in deionized water for 24 h at room temperature.

Conversion rate of monomer was calculated by the following calculation, Formula (2):

$$Y = \frac{G - GA}{GB} \quad (2)$$

Y (g): Conversion rate of the monomer

G (g) : Weight of the sample.
A (g) : Percentage of non-volatile components with the exception of monomers.
B (g) : Percentage of monomers in the formula.

3. Results

Morphology of WPUA-40 colloidal particles is shown in Figure 1 using TEM with different magnification times. As we can see from Figure 1, colloidal particles exhibited distinct dark and light domains with clear boundaries, indicating that the core-shell structure was formed. Due to the different polarities of WPU and MMA, MMA was preferably confined to the core region during the copolymerization process. Therefore, the light domains represent WPU, and the dark domains represent MMA.

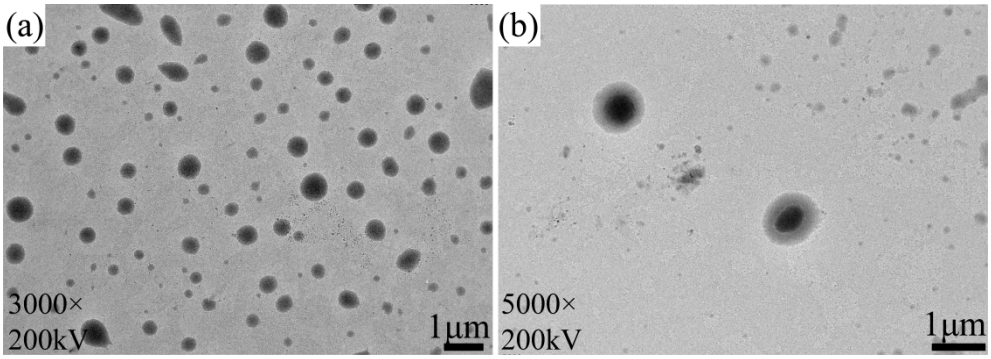

Figure 1. TEM image of WPUA colloidal particles. (**a**) TEM image of WPUA colloidal particles at 3000× magnification. (**b**) TEM image of WPUA colloidal particles at 5000× magnification.

Figure 2 illustrated the thermal stability of the WPU, WPUA-10, WPUA-20, WPUA-30, and WPUA-40 coatings. The decomposition of the coating was divided into two stages. The first stage was from the initial temperature (25 °C) to 220 °C, and the loss of sample weight was because of the residual water and small molecular solvents in the coating. The second stage is the decomposition of the polymer. As we can see in Figure 2, with the increase of MMA content, the thermogravimetric analysis curve obviously shifted to the right, indicating that the thermal resistance of the coating was significantly improved. The reason is that the polymerization reaction between MMA and polyurethane increased the cross-linking degree. This effective cross-linking structure enhances the force between molecular chains, resulting in a better thermal resistance of WPUA coatings.

From the particle size analysis results of WPU and WPUA emulsions, the average particle size of a WPU emulsion was 66.49 nm; WPUA-10 was 67.75 nm, WPUA-20 was 74.1 nm, WPUA-30 was 142 nm, and WPUA-40 was 162 nm, respectively.

The particle size distribution curves of emulsions with different MMA content are shown in Figure 3. As we can see from Figure 3, the average particle size of the WPU emulsion was the smallest with a narrow distribution, indicating that the particle size of WPU was uniform. For WPUA emulsion, there was no significant change in the particle size distribution of WPUA-10 and WPUA-20. As the content of MMA increased to 30%, the average particle size of the WPUA-30 increased to 142 nm, and the particle size distribution became wider when compared with WPU, WPUA-10, and WPUA-20. The reason may be that with the increase of MMA content, more and more MMA monomer was swollen into the core-shell structure for copolymerization, and the WPU colloidal particle surface was stretched, resulting in bigger particle size. As the sample of WPUA-40, the particle size distribution ranged from 50 to 600 nm. The reason is that excessive MMA content is swollen into the core structure, leading to high surface inflation of the WPUA colloidal particle, which contributed to the poor self-emulsifying ability of the WPUA colloidal particle, resulting in higher particle size and colloidal sedimentation.

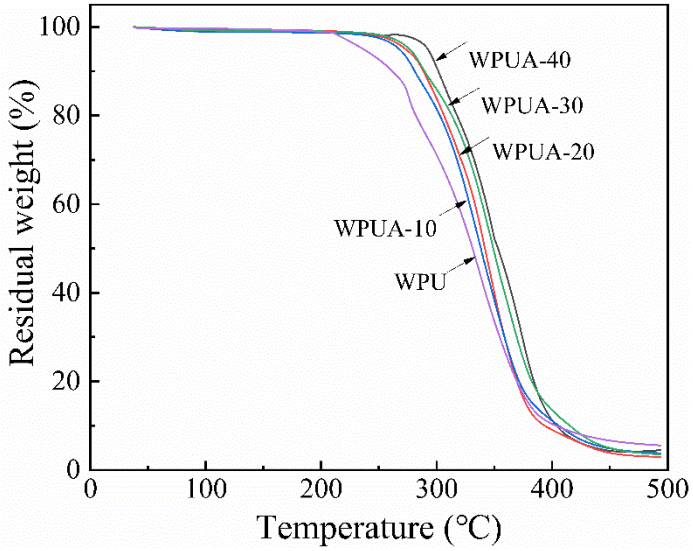

Figure 2. Thermogravimetric curves of WPU, WPUA-10, WPUA-20, WPUA-30, and WPUA-40 coatings.

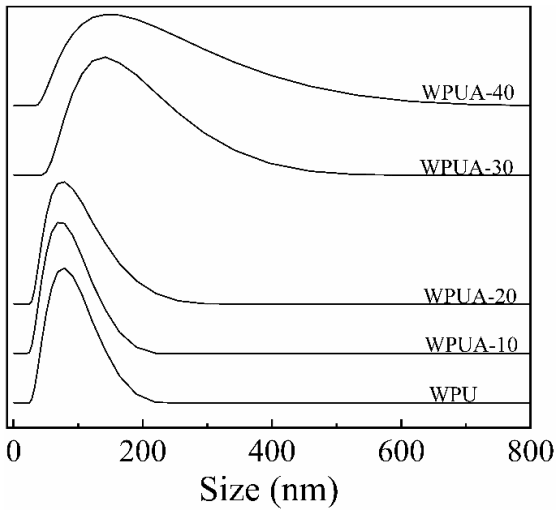

Figure 3. Particle size distribution of WPU and WPUA-10, WPUA-20, WPUA-30, and WPUA-40 emulsion.

Figure 4 illustrates the monomer conversion with reaction time utilizing the batch and semi-batch emulsion polymerization method, and WPUA-10 was selected as the experimental sample. It is observed from Figure 4 that the monomer conversion reached the maximum value of 96% at 180 min in terms of semi-batch emulsion polymerization, and 84.2% at 150 min in terms of batch emulsion polymerization. Compared with the semi-bath emulsion polymerization, the bath emulsion polymerization period was shorter with lower monomer conversion. The reason is that high initial monomer concentration leads to vigorous polymerization with serious reflux phenomena during the batch emulsion polymerization process; a large number of gel particles were found on the wall of the four-necked flask, resulting in a low monomer conversion rate. In the semi-bath reaction process, KPS solution was added into flask drop by drop to keep the concentration of the initiator in the system at a low level so the reaction could proceed smoothly, resulting in lower gel fractions and higher monomer conversions.

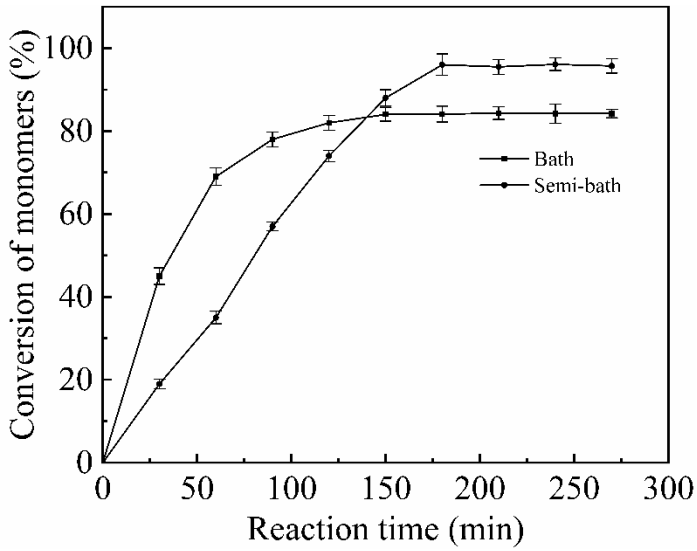

Figure 4. Effect of the polymerization method on the conversion of the monomer.

The characteristics of coatings such as water absorption, pencil hardness, and appearance are the crucial factors for fabricating inkjet inks. Table 2 illustrates the coating properties of WPU, WPUA-10, WPUA-20, WPUA-30, and WPUA-40. It is observed that from Table 2 with the MMA content increasing from 0% to 40%, the water absorption of the prepared coatings decreased from 23.5% to 13%, and the pencil hardness was enhanced from HB to 3H. The appearance of the prepared coatings with the MMA content from 0% to 30% was transparent, and the sample with MMA content of 40% was translucent. The reason for the above experimental results is that MMA as a hard monomer is incorporated into the molecular chains, resulting in more cross-linking sites between polyurethane and acrylate, which limits the movement of the molecular chains. Therefore, the prepared coatings exhibited a compact structure and higher strength, and it is difficult for water to penetrate and swell the prepared coatings.

Table 2. Properties of the WPU and WPUA coatings.

Sample	**Properties**		
Emulsion	**Water Absorption (%)**	**Pencil Hardness**	**Appearance**
WPU	23.5	HB	Transparent
WPUA-10	21	H	Transparent
WPUA-20	18.2	2H	Transparent
WPUA-30	15	2H	Transparent
WPUA-40	13	3H	Translucent

The appearance of the emulsion is usually related to the light scattering and absorption by the dispersed phase and dispersion medium. From the particle size distribution results in Figure 3, the average colloidal particle size became bigger with the increasing of MMA content. With the particle size of the colloidal particles increased, the total internal reflection occurred and decreased the transparency of emulsion and the appearance was white. The change appearance of the emulsion shown in Table 2 validates the particle size distribution results in Figure 3.

The contact angle (CA) of emulsion on a solid surface is an important parameter to measure the wettability of the emulsion. A low CA (<90°) of emulsion corresponds to a better wettability. Conversely, a high CA (>90°) implies poor wettability of the emulsion. For inkjet printing, the CA of inkjet ink has a significant impact on printing quality. The

inkjet ink with low CA easily infiltrates onto the substrate and improves the printing quality. On the contrary, it is difficult for the ink droplets to infiltrate into the substrate, resulting in interruption of the printing pattern.

In order to define the effect of MMA content on the wettability of WPUA emulsions, a neat glass plate was selected as the substrate during contact angle analysis. To avoid the influence of other factors, all emulsions were configured to a uniform solid content before testing.

As we can see from Figure 5, the CA of WPU (46°) was higher than that of the WPUA emulsion. This phenomenon is attributed to the addition of SDS during the preparation of the WPUA emulsion, which improves the wettability of WPUA on the glass plate surface. It is worth noting that the contact angle of the emulsion was increased with the increasing of MMA content: 31.9° for WPUA-10, 36.4° for WPUA-20, 38.1° for WPUA-30, and 42.9° for WPUA-40. The reason is that MMA as a polar monomer was introduced into the WPU backbone, which improved the cross-linking degree between segments, reflecting the increase of CA.

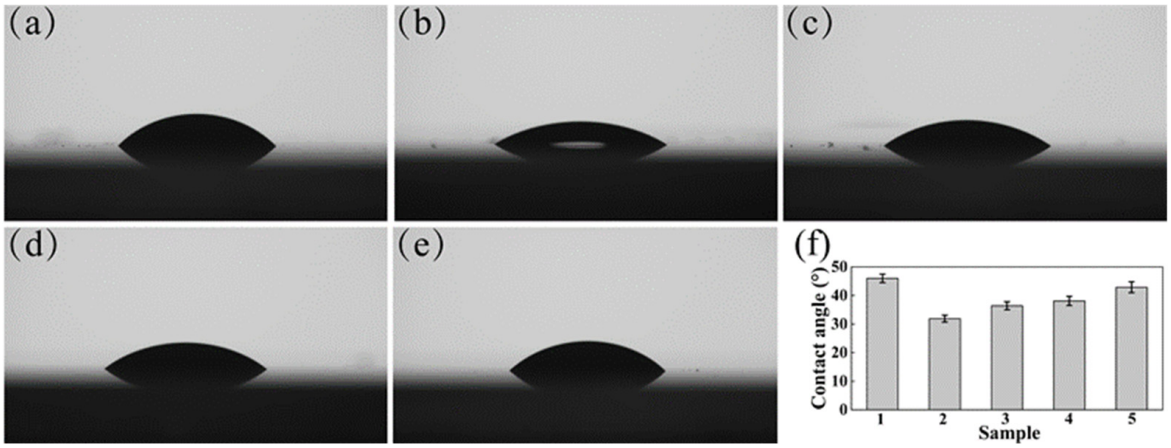

Figure 5. Contact angle analysis of WPU and WPUA emulsion. (**a**–**e**) Contact angle images of WPU, WPUA-10, WPUA-20, WPUA-30, and WPUA-40. (**f**) Schematic diagram illustrating the contact angles of WPU and WPUA emulsions. The numbers 1, 2, 3, 4, and 5 inserted in f represent WPU, WPUA-10, WPUA-20, WPUA-30, and WPUA-40, respectively.

The inkjet printing color blocks and corresponding ΔE are exhibited in Figure 6. In this section, WPUA-20 was selected as the binder resin to prepare the inkjet ink. As we know, CMYK as the basic color in the inkjet printing can be deployed to obtain a variety of colors so as to achieve full-color printing. In order to define the adaptability of WPUA emulsion in the field of inkjet printing, we prepared C, M, Y, and K inkjet printing ink and tested its printability. From Figure 6a, the outputting color blocks were colorful and neat in appearance, indicating that the WPUA emulsion has good encapsulation and transfer ability for pigments. From Figure 5b, the biggest ΔE of the sample was yellow (ΔE = 0.39), the smallest ΔE of the sample was magenta (ΔE = 0.32), and the ΔE of all the color blocks was between 0.3 and 0.5, indicating that the color development performance of the inkjet ink is good. It is worth mentioning that after a long time of printing, it could still print smoothly. The above results further prove that the prepared inkjet ink has good printability and the compatibility between WPUA and pigments is good.

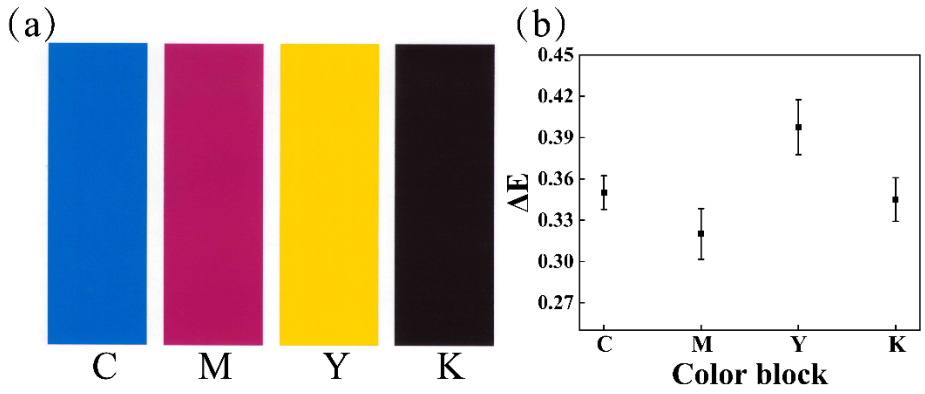

Figure 6. Inkjet printing color block and ΔE. (**a**) The prepared inkjet printing color block, (**b**) ΔE of inkjet printing color block. The inserted C, M, Y, and K represent cyan, magenta, yellow, and black, respectively.

4. Conclusions

A core-shell WPUA emulsion with different MMA content was synthesized by the emulsion polymerization method with WPU as seeds. The morphology of core-shell WPUA colloidal particle was detached by TEM with WPU as the shell and MMA as the core. With the increase of MMA content in WPUA, the average particle size and CA of WPUA emulsion increased, and the thermal resistance and hardness of the WPUA coating was enhanced. The prepared inkjet printing ink using WPUA emulsion as the binder resin showed good printability.

Author Contributions: Conceptualization, X.W.; data curation, X.W. and J.W.; formal analysis, Y.F.; investigation, X.W.; methodology, X.W.; project administration, F.C.; supervision, X.W. and J.W.; writing—original draft, X.W.; writing—review and editing, X.W. All authors have read and agreed to the published version of the manuscript.

Funding: This research was funded by the National Natural Science Foundation of China (No. 52075435).

Institutional Review Board Statement: Not applicable.

Informed Consent Statement: Not applicable.

Data Availability Statement: Not applicable.

Conflicts of Interest: The authors of this article have no conflict of interest.

References

1. Wu, J.; Cui, C.; Guo, X. Impacts of the West–East Gas Pipeline Project on energy conservation and emission reduction: Empirical evidence from Hubei province in Central China. *Environ. Sci. Pollut. Res.* **2022**, *29*, 28149–28165. [CrossRef] [PubMed]
2. Zhu, Q.; Li, X.; Li, F.; Zhou, D. The potential for energy saving and carbon emission reduction in China's regional industrial sectors. *Sci. Total Environ.* **2020**, *716*, 135009. [CrossRef] [PubMed]
3. Liu, X.; Hong, W.; Chen, X. Continuous Production of Water-Borne Polyurethanes: A Review. *Polymers* **2020**, *12*, 2875. [CrossRef]
4. López-garcía, J.; Lehocký, M.; Junkar, I.; Mozeti, M.; Sowe, M. Enhanced printability of polyethylene through air plasma treatment. *Vacuum* **2013**, *95*, 43–49. [CrossRef]
5. Kim, M.K.; Jeong, W.; Lee, S.M.; Kim, J.B.; Jin, S.; Kang, H.-W. Decellularized extracellular matrix-based bio-ink with enhanced 3D printability and mechanical properties. *Biofabrication* **2020**, *12*, 025003. [CrossRef] [PubMed]
6. Oliveira, S.M.; Fasolin, L.H.; Vicente, A.A.; Fuciños, P.; Pastrana, L.M. Printability, microstructure, and flow dynamics of phase-separated edible 3D inks. *Food Hydrocoll.* **2020**, *109*, 106120. [CrossRef]
7. Yang, X.; Wei, X.F.; Huang, B.Q.; Zhang, W.; Zhao, L. Study on the Printability of UV-Curable Inkjet Ink on Different Printed Materials. *Adv. Print. Packag. Technol.* **2013**, *262*, 324–328. [CrossRef]
8. Aigbodion, A.I.; Pillai, C.K.S. Preparation, analysis and applications of rubber seed oil and its derivatives in surface coatings. *Prog. Org. Coat.* **2000**, *38*, 187–192. [CrossRef]
9. Ates, B.; Koytepe, S.; Karaaslan, M.G.; Balcioglu, S.; Gulgen, S. Biodegradable non-aromatic adhesive polyurethanes based on disaccharides for medical applications. *Int. J. Adhes. Adhes.* **2014**, *49*, 90–96. [CrossRef]

10. Han, Y.; Hu, J.; Xin, Z. Facile preparation of high solid content waterborne polyurethane and its application in leather surface finishing. *Prog. Org. Coat.* **2019**, *130*, 8–16. [CrossRef]
11. Khojasteh-Khosro, S.; Shalbafan, A.; Thoemen, H. Consumer behavior assessment regarding lightweight furniture as an environmentally-friendly product. *Wood Mater. Sci. Eng.* **2022**, *17*, 192–201. [CrossRef]
12. An, X.; Shen-wei, M.; Tian-jiang, C.; Hui, Y.; Ming, Z. Microstructure and properties of cerium oxide / polyurethane elastomer composites. *Rare Metals.* **2021**, *40*, 3685–3693.
13. Chung, Y.C.; Park, J.E.; Choi, J.W.; Chun, B.C. The grafting of phthalic acid onto polyurethane copolymer and its impact on the surface hydrophilicity, tensile stress, and shape recovery properties. *J. Macromol. Sci. Part A* **2019**, *56*, 577–587. [CrossRef]
14. Zhong, X.; Lv, L.; Hu, H.; Jiang, X.; Fu, H. Bio-based coatings with liquid repellency for various applications. *Chem. Eng. J.* **2020**, *382*, 123042. [CrossRef]
15. Hu, J.L.; Mondal, S. Structural characterization and mass transfer properties of segmented polyurethane: Influence of block length of hydrophilic segments. *Polym. Int.* **2005**, *54*, 764–771. [CrossRef]
16. Son, S.-H.; Lee, H.-J.; Kim, J.-H. Effects of carboxyl groups dissociation and dielectric constant on particle size of polyurethane dispersions. Colloids and Surfaces A. *Physicochem. Eng. Asp.* **1998**, *133*, 295–301. [CrossRef]
17. Białkowska, A.; Bakar, M.; Marchut-Mikołajczyk, O. Biodegradation of linear and branched nonisocyanate condensation polyurethanes based on 2-hydroxy-naphthalene-6-sulfonic acid and phenol sulfonic acid. *Polym. Degrad. Stab.* **2019**, *159*, 98–106. [CrossRef]
18. Luo, S.L.; Gong, G.F.; Deng, J.Q.; Shi, G.; Zhu, H. Improved Water Resistance of Waterborne Polyurethane. *Adv. Mater. Res.* **2010**, *168–170*, 1796–1800. [CrossRef]
19. Ligon-Auer, S.C.; Schwentenwein, M.; Gorsche, C.; Stampfl, J.; Liska, R. Toughening of photo-curable polymer networks: A review. *Polym. Chem.* **2016**, *7*, 257–286. [CrossRef]
20. Akarsu Dulgar, C.; Çakır Çanak, T.; Serhatlı, I.E. Effect of boron acrylate monomer content and multi-acrylate functional boron methacrylate on adhesive performance for water-borne acrylic polymers. *Polym. Bull.* **2019**, *76*, 2499–2517. [CrossRef]
21. Aalto-Korte, K.; Alanko, K.; Kuuliala, O.; Jolanki, R. Occupational methacrylate and acrylate allergy from glues. *Contact Dermat.* **2008**, *58*, 340–346. [CrossRef] [PubMed]
22. Qiu, F.X.; Zhang, J.L.; Wu, D.M.; Yang, D.Y. Waterborne polyurethane and modified polyurethane acrylate composites. *Plast. Rubber Compos.* **2010**, *39*, 454–459. [CrossRef]
23. Vlad, S. Some interpenetrating polymer networks based on polyurethane and polyurethane acrylate. *Mater. Plast.* **2002**, *39*, 137–141.
24. Guo, S.; Zou, Y.; He, J.; Liu, F. Study on synthesis, characterizations, and properties of pyridinol-blocked isocyanates and waterborne polyurethane. *Int. J. Polym. Anal. Charact.* **2016**, *21*, 708–717. [CrossRef]
25. Zheng, J.; Nie, Q.; Guan, H.; Wu, X.; Zhang, S.; Wu, J.; Wang, Z.; Zhang, S. A novel waterborne fluorinated polyurethane–acrylate film for ultraviolet blocking and antiprotein fouling. *J. Coat. Technol. Res.* **2021**, *18*, 1295–1307. [CrossRef]